

Jet substructure shedding light on heavy Majorana neutrinos at the LHC

Arindam Das,^a Partha Konar,^b and Arun Thalapillil^c

^a*School of Physics, KIAS, Seoul 130-722, Korea*

^b*Theoretical Physics Group, Physical Research Laboratory, Ahmedabad-380009, India*

^c*Indian Institute of Science Education and Research, Homi Bhabha Rd, Pashan, Pune 411 008, India*

E-mail: arindam@kias.re.kr, konar@prl.res.in,
thalapillil@iiserpune.ac.in

ABSTRACT: The existence of tiny neutrino masses and flavor mixings can be explained naturally in various seesaw models, many of which typically having additional Majorana type SM gauge singlet right handed neutrinos (N). If they are at around the electroweak scale and furnished with sizeable mixings with light active neutrinos, they can be produced at high energy colliders, such as the Large Hadron Collider (LHC). A characteristic signature would be same sign lepton pairs, violating lepton number, together with light jets – $pp \rightarrow N\ell^\pm$, $N \rightarrow \ell^\pm W^\mp$, $W^\mp \rightarrow jj$. We propose a new search strategy utilising jet substructure techniques, observing that for a heavy right handed neutrino mass M_N much above M_{W^\pm} , the two jets coming out of the boosted W^\pm may be interpreted as a single fat-jet (J). Hence, the distinguishing signal topology will be $\ell^\pm\ell^\pm J$. Performing a comprehensive study of the different signal regions along with complete background analysis, in tandem with detector level simulations, we compute statistical significance limits. We find that heavy neutrinos can be explored effectively for mass ranges $300 \text{ GeV} \leq M_N \leq 800 \text{ GeV}$ and different light-heavy neutrino mixing $|V_{\mu N}|^2$. At the 13 TeV LHC with 3000 fb^{-1} integrated luminosity one can competently explore mixing angles much below present LHC limits, and moreover exceed bounds from electroweak precision data.

KEYWORDS: Large Hadron Collider, Seesaw neutrino mass, Jet substructure.

Contents

1	Introduction	1
2	Model and heavy Majorana neutrinos at the LHC	3
3	Fat-jets and Jet Substructure for W-like jet tagging	6
4	Analysis setup and Simulation	7
5	Results and Discussion	10
6	Conclusions	14

1 Introduction

The experimental evidence for neutrino oscillations [1–6] and lepton flavor mixings, from the various experiments, motivate extensions of the SM incorporating non-zero neutrino masses and mixings. After the pioneering realization of the unique $d = 5$ operator [7] within the SM with $\Delta L = 2$ lepton number violation ($L =$ Lepton number), it was realized that the Seesaw mechanism [8–14] could be the simplest idea to explain the smallness of the neutrino masses and flavor mixings. In many of these models, SM is extended by gauge singlet, Majorana type, heavy right handed neutrinos (RHNs). After electroweak (EW) symmetry breaking, the light Majorana neutrino masses are generated by, for instance, the so called type-I seesaw mechanism.

Through the seesaw mechanism, the flavor eigenstates of the SM light neutrino mix with the mass eigenstates of the light neutrinos and RHNs. The SM singlet RHNs (N) interact with the SM gauge bosons through lepton mixing. Such Majorana type RHNs, if at the EW scale, can be produced at the Large Hadron Collider (LHC) with a distinguishing signature – Same Sign Di-Leptons (SSDL) and di-jets. In this channel the heavy RHNs decay into a W^\pm and a lepton. In cases where the RHNs are sufficiently massive, very often the gauge bosons are significantly boosted, resulting in collimated energy deposits in the hadronic calorimeter. With a suitable jet algorithm, these collimated hadron four momenta may be reconstructed as a fat-jet (J). Fat-jets retain information of their origins and have several distinct properties that may be leveraged for tagging and signal discrimination. The resulting signal of interest therefore becomes SSDL + fat-jet. In this paper we consider searches for RHNs with masses $M_N \geq 300$ GeV, which is sufficient to produce boosted jets. It is important

to search for such relatively small-mass RHNs at colliders, since from a very general theoretical viewpoint, a small M_N may be considered technically natural [15, 16]. This is because in the limit $M_N \rightarrow 0$ one regains $U(1)_{B-L}$ as a global symmetry of the Lagrangian. Different experiments such as ATLAS [17] and CMS [18, 19] have already searched for RHNs in the SSDL + dijets channel, assuming non-boosted W^\pm .

At the 8 TeV LHC, with 20.3 fb^{-1} luminosity and 95% confidence limit (C. L.), ATLAS [17] has probed mixings for muon flavor down to a $|V_{\mu N}|^2$ of 3.5×10^{-3} , for $M_N = 100 \text{ GeV}$. The limits further goes down to 2.9×10^{-3} for $M_N = 110 \text{ GeV}$ and then monotonically weakens with mass, up to $M_N = 500 \text{ GeV}$. At $M_N = 500 \text{ GeV}$ the limits are $|V_{\mu N}|^2 = 4 \times 10^{-1}$. The limits are nearly two orders of magnitude weaker in the case of electron flavor mixings $|V_{eN}|^2$ at the 95% C. L.

CMS has also studied the SSDL plus dijet signal and obtain the exclusion limits for $|V_{eN}|^2$ [18] and $|V_{\mu N}|^2$ [19]. Both studies are performed at the 8 TeV LHC with 19.7 fb^{-1} luminosity at 95% C. L. The limits for the mixed $e^\pm \mu^\pm + jj$ final state was also considered in [18]. CMS observed upper limits for $|V_{eN}|^2$ at 1.2×10^{-4} for $M_N = 40 \text{ GeV}$, 2×10^{-2} for $M_N = 85 \text{ GeV}$, 8×10^{-3} for $M_N = 130 \text{ GeV}$ and 1.2×10^{-2} for $M_N = 200 \text{ GeV}$. Thus, the $|V_{eN}|^2$ limits were found to again weaken with M_N . Alternatively, RHNs may be excluded as large as $M_N = 480 \text{ GeV}$, assuming the mixing is unity. The limits on $|V_{\mu N}|^2$ from the SSDL + dijet final state with μ flavor is probed down to 2×10^{-5} for $M_N = 40 \text{ GeV}$, 4.5×10^{-3} for $M_N = 90 \text{ GeV}$, 1.75×10^{-3} for $M_N = 125 \text{ GeV}$ and 7×10^{-3} for $M_N = 175 \text{ GeV}$ with $|V_{\mu N}|^2$ again weakening subsequently with M_N . For $M_N = 500 \text{ GeV}$ the limit is $|V_{\mu N}|^2 = 0.6$.

In this paper we leverage boosted W^\pm production from massive RHN, and its subsequent decay into a fat-jet in association with $\mu^\pm \mu^\pm$ pairs. The P_T of the W^\pm scale as $P_T^W \sim (M_N^2 - M_W^2)/M_N$ and the separation between the hadronic decay products of W^\pm scale as $\sim M_W/P_T^W$. Therefore, a natural region of focus may be the intermediate to heavy RHN mass range, say $M_N \geq 300 \text{ GeV}$. In this mass range, the only other competent limit that exists comes from indirect EW precision data (EWPd). The EWPd limit is around $|V_{\mu N}|^2 = 0.009$ [20, 21, 23]. The mixing limits may also be obtained from the Higgs data [24–26] for $10 \text{ GeV} \leq M_N \leq 200 \text{ GeV}$.

For simplicity and clarity, we consider only the μ flavor for the SSDL. Moreover, μ detection efficiencies are better, compared to electrons and tau leptons. We place limits on $|V_{\mu N}|^2$ at the 13 TeV LHC, with 3000 fb^{-1} luminosity, in the $300 \text{ GeV} \leq M_N \leq 800 \text{ GeV}$ mass range. A representative diagram for the parton level production and decay of RHN, leading to final states of interest, is shown in figure 1.

Search strategies utilising boosted and collimated objects have proven to be spectacularly successful in searches at the LHC. The seminal ideas [27–30] have burgeoned into many sophisticated methods that enable tagging jets arising from the decay of boosted heavy particles, improving searches for new topologies, investigating jet properties and mitigating underlying events and pile-up (please see [31] and references therein for a review of some these techniques).

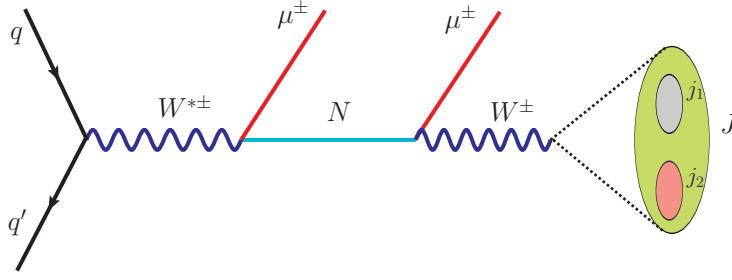


Figure 1. SSDL + fat-jet production at the LHC.

In the context of sterile neutrinos and related models there have been a few studies that have, in a broader sense, leveraged the effectiveness of collimated objects in the signal topology [32–36]. Nevertheless, surprisingly, there have not been any investigations in the SSDL+fat-jet channel, in the RHN collider search context. We utilise for the first time, jet substructure techniques to augment RHN searches, in the $l^\pm l^\pm J$ channel corresponding to figure 1.

The paper is organized as follows. In section 2, we discuss the prototypical model along with the RHN production cross sections at the 13 TeV LHC. We also calculate the decay widths and the corresponding branching ratios there. In section 3, we briefly describe the fat-jet technique for W-tagging. Sections 4 and 5 are dedicated to the setup, collider analysis, discussion of kinematic distributions, and presentation of the salient results and limits. We conclude in section 6.

2 Model and heavy Majorana neutrinos at the LHC

In the simplest model of seesaw, we only introduce SM gauge-singlet Majorana RHNs N_R^β (where β is a flavor index). N_R^β would couple with the SM lepton doublet ℓ_L^α and the Higgs doublet H . The relevant part of the Lagrangian density is

$$\mathcal{L} \supset -Y_D^{\alpha\beta} \bar{\ell}_L^\alpha H N_R^\beta - \frac{1}{2} M_N^{\alpha\beta} \bar{N}_R^{\alpha C} N_R^\beta + H.c.. \quad (2.1)$$

After EW symmetry breaking by a vacuum expectation value (VEV) $H = \left(\frac{v}{\sqrt{2}} \ 0\right)^T$, we obtain the Dirac mass matrix $M_D = \frac{Y_D v}{\sqrt{2}}$. Using these Dirac and Majorana mass matrices, we can write the full neutrino mass matrix as

$$M_\nu = \begin{pmatrix} 0 & M_D \\ M_D^T & M_N \end{pmatrix}. \quad (2.2)$$

Diagonalizing this matrix, we obtain the well-known seesaw formula for the light Majorana neutrinos

$$m_\nu \simeq -M_D M_N^{-1} M_D^T. \quad (2.3)$$

With $M_N \sim 100$ GeV, we require $Y_D \sim 10^{-6}$ for $m_\nu \sim 0.1$ eV. However, in the general parameterization for the seesaw formula [37], Y_D can be large and sizable, which is the case we are going to consider in this paper. An interesting class of models have mass matrices M_D and M_N with specific textures, enforced by some symmetries [85, 90–95], so that a large light-heavy neutrino mixing occurs even at a low scale, satisfying the neutrino oscillation data.

If these RHNs reside at the electroweak scale, then they can be produced in high energy colliders such as the LHC [38–76]. Searches for Majorana RHNs can be performed via the ‘smoking-gun’ tri-lepton, as well as, SSDL+dijet signals. The rates will generally be suppressed by the square of light-heavy mixing $|V_{\ell N}|^2 \simeq |M_D M_N^{-1}|^2$. A comprehensive, general study¹ of $|V_{\ell N}|^2$ and associated parameters is given in [77]. Bounds may be placed on the light-heavy mixing angles using results from different experiments, as in [17–26, 81, 87], considering degenerate Majorana RHNs.

Through the seesaw mechanism, a flavor eigenstate (ν) of the SM neutrino may be expressed in terms of the mass eigenstates of the light (ν_m) and heavy (N_m) Majorana neutrinos as

$$\nu \simeq \mathcal{N}\nu_m + \mathcal{R}N_m. \quad (2.4)$$

Here

$$\mathcal{R} = M_D M_N^{-1}, \quad \mathcal{N} = \left(1 - \frac{1}{2}\epsilon\right) U_{\text{PMNS}}, \quad (2.5)$$

with $\epsilon = \mathcal{R}^* \mathcal{R}^T$ and U_{PMNS} [88, 89] the usual neutrino mixing matrix. In terms of mass eigenstates, the charged current interactions for the heavy neutrinos is then given by

$$\mathcal{L}_{CC} = -\frac{g}{\sqrt{2}} W_\mu \bar{e} \gamma^\mu P_L (\mathcal{N}\nu_m + \mathcal{R}N_m) + h.c., \quad (2.6)$$

where e denotes three generations of charged leptons, in vector form, and $P_L = \frac{1}{2}(1 - \gamma_5)$. Similarly, the neutral current interactiona are given by

$$\begin{aligned} \mathcal{L}_{NC} = & -\frac{g}{2c_w} Z_\mu \left[\bar{\nu}_m \gamma^\mu P_L (\mathcal{N}^\dagger \mathcal{N}) \nu_m + \bar{N}_m \gamma^\mu P_L (\mathcal{R}^\dagger \mathcal{R}) N_m \right. \\ & \left. + \left\{ \bar{\nu}_m \gamma^\mu P_L (\mathcal{N}^\dagger \mathcal{R}) N_m + h.c. \right\} \right], \end{aligned} \quad (2.7)$$

where $c_w = \cos \theta_w$ with θ_w being the weak mixing angle.

At the LHC, the heavy neutrinos can be produced through charged current interactions, via the s -channel exchange of W bosons. The main production process

¹The study uses data from neutrino oscillation experiments [1–6], bounds from Lepton Flavor Violation (LFV) [78–80], Large Electron-Positron (LEP) [20, 23, 81] experiments using the non-unitarity effects [82, 83] applying the Casas- Ibarra conjecture [37, 58, 85, 86].

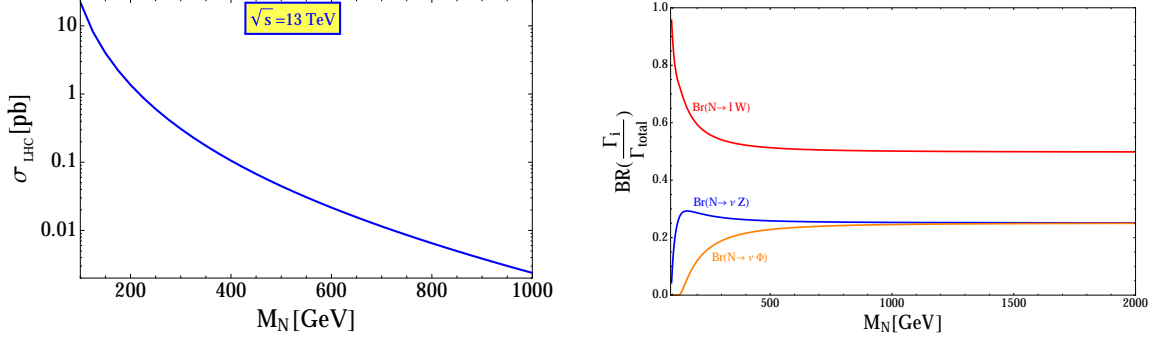


Figure 2. (Left) The total production cross section of the heavy Majorana neutrino as a function of its mass at the LHC with $\sqrt{s} = 13$ TeV and normalised by the $|V_{\mu N}|^2$. (Right) Heavy neutrino branching ratios (BR_i) for different decay modes as a function of its mass.

at the parton level is $u\bar{d} \rightarrow \mu^+ N$ (and $\bar{u}d \rightarrow \mu^- N$). The differential cross section is found to be

$$\frac{d\hat{\sigma}_{LHC}}{d\cos\theta} = (3.89 \times 10^8 \text{ pb}) \times \frac{\beta}{32\pi\hat{s}} \frac{\hat{s} + M_N^2}{\hat{s}} \left(\frac{1}{2}\right)^2 3 \left(\frac{1}{3}\right)^2 \frac{g^4}{4} \frac{(\hat{s}^2 - M_N^4)(2 + \beta \cos^2\theta)}{(\hat{s} - M_W^2)^2 + M_W^2 \Gamma_W^2}, \quad (2.8)$$

where $\sqrt{\hat{s}}$ is the center-of-mass energy of the colliding partons, M_N the mass of N , and $\beta = (\hat{s} - M_N^2)/(\hat{s} + M_N^2)$. The total production cross section at the LHC is thus given by

$$\sigma_{LHC} = \int d\sqrt{\hat{s}} \int d\cos\theta \int_{\hat{s}/E_{CMS}^2}^1 dx \frac{\sqrt{4\hat{s}}}{xE_{CMS}^2} f_u(x, Q) f_{\bar{d}}\left(\frac{\hat{s}}{xE_{CMS}}, Q\right) \frac{d\hat{\sigma}_{LHC}}{d\cos\theta} + (u \rightarrow \bar{u}, \bar{d} \rightarrow d). \quad (2.9)$$

We take $E_{CMS} = 13$ TeV, for the center-of-mass energy of the LHC. In the numerical analysis, we further employ CTEQ5M [111] for the u -quark (f_u) and \bar{d} -quark ($f_{\bar{d}}$) parton distribution functions, with a factorization scale $Q = \sqrt{\hat{s}}$. The total cross section thus computed, as a function of M_N , is depicted in figure 2 (Left pane), normalized by $|V_{\mu N}|^2$. Hence, the resultant cross sections shown in figure 2 correspond to maximum values for a fixed M_N .

The main decay modes of the heavy neutrino are $N \rightarrow \ell W$, $\nu_\ell Z$, $\nu_\ell h$. The corresponding partial decay widths [43–45, 97, 98] are given by

$$\begin{aligned} \Gamma(N \rightarrow \ell W) &= \frac{g^2 |V_{\ell N}|^2 (M_N^2 - M_W^2)^2 (M_N^2 + 2M_W^2)}{64\pi M_N^3 M_W^2}, \\ \Gamma(N \rightarrow \nu_\ell Z) &= \frac{g^2 |V_{\ell N}|^2 (M_N^2 - M_Z^2)^2 (M_N^2 + 2M_Z^2)}{128\pi c_w^2 M_N^3 M_Z^2}, \\ \Gamma(N \rightarrow \nu_\ell h) &= \frac{|V_{\ell N}|^2 (M_N^2 - M_h^2)^2}{32\pi M_N} \left(\frac{1}{v}\right)^2. \end{aligned} \quad (2.10)$$

Note that the decay width of heavy neutrinos into W^\pm is about twice as large as that into Z^0 , owing to the two degrees of freedom. We plot the branching ratios $BR_i (\equiv \Gamma_i/\Gamma_{\text{total}})$ of the various decay modes (Γ_i) in figure 2 (Right pane). Note that for larger values of M_N , the branching ratios are related as

$$BR(N \rightarrow \ell W) : BR(N \rightarrow \nu Z) : BR(N \rightarrow \nu H) \simeq 2 : 1 : 1. \quad (2.11)$$

As mentioned earlier, in our analysis we will consider Majorana RHNs having mass in the range $300 \text{ GeV} \leq M_N \leq 800 \text{ GeV}$. In this mass range, the W^\pm boson from the leading decay mode $N \rightarrow \ell W$ (see figure 2), will be boosted. These boosted W^\pm can decay hadronically to produce a fat-jet, with the characteristic final state $\mu^\pm \mu^\pm J$.

3 Fat-jets and Jet Substructure for W -like jet tagging

As we have emphasized, in scenarios where the right-handed neutrino is very heavy, the hadronically decaying daughter W^\pm will typically have a large boost. This causes the jets from the W^\pm to be very collimated and one would detect them as a single jet – a ‘fat-jet’ (J). The boosted topology and its associated substructure is extremely powerful in reducing backgrounds, mitigating underlying event contamination and in event tagging [31]. In our context, the jet substructure analysis primarily appears as a means to efficiently tag the hadronically decaying boosted- W^\pm . Our strategy will be to leverage two variables – N-subjettiness and jet-mass – to achieve efficient W -tagging in the $\mu^\pm \mu^\pm J$ final state.

N-subjettiness [99, 100] is an inclusive jet shape variable defined as

$$\tau_N = \frac{1}{\mathcal{N}_0} \sum_i p_{i,T} \min \{ \Delta R_{i1}, \Delta R_{i2}, \dots, \Delta R_{iN} \}. \quad (3.1)$$

The normalization is defined as $\mathcal{N}_0 = \sum_i p_{i,T} R$. i runs over the constituent particles in the jet. $p_{i,T}$ are transverse momenta of the constituent particles, $\Delta R_{i\alpha} = \sqrt{(\Delta\eta)_{i\alpha}^2 + (\Delta\phi)_{i\alpha}^2}$ is the $\eta - \phi$ distance between a candidate α -subjet and a constituent particle i and R is the jet radius. τ_N tries to quantify if the original jet consists of N daughter subjets. A low value of τ_N suggests that the original jet consists of N or fewer daughter subjets. Thus, information from τ_N may potentially be used to identify an object that has an N -prong hadronic decay. In fact, it has been shown that a better discriminant to tag an N -subjet object is to consider ratios τ_N/τ_{N-1} [99, 100]. For W -tagging, the W^\pm yields two subjets that are collimated, and hence the variable of interest is $\tau_{21}^J = \tau_2/\tau_1$. The mass of the fat-jet (M_J), after suitable jet grooming, is another variable that can help in distinguishing signal events from background. At each iteration in a sequential recombination jet algorithm, in the E-scheme, the mother proto jet four-momentum is the vector sum of the daughter

proto jet four-momenta. In this fashion, the jet algorithm at the end of the iteration provides a P_T^J for the full fat-jet. M_J^2 is computed as the invariant mass square of the fat-jet four momentum (P_J^2).

To reconstruct the candidate fat-jet, **Delphes** 3.3.2 [101] hadron calorimeter outputs are clustered using **FastJet** 3.1.3 [102, 103]. The τ_{21}^J is computed with the aid of the N-subjettiness extension, available as part of the **FastJet-contrib** [102, 103]. Following [104] for W-tagging, we will choose for the jet clustering algorithm Cambridge-Aachen [105, 106] with a jet-cone radius $R = 0.8$. We will in addition require specific cuts on τ_{21}^J and M_J for efficient W-tagging, as we shall discuss in section 5.

4 Analysis setup and Simulation

In preparation for our exploration of the SSDL+fat-jet channel at 13 TeV LHC, along with establishing the setup in terms of signal RHN model files and a jet substructure analysis strategy, we must also consider the relevant backgrounds carefully. Towards this end we will perform detailed background simulations and study the prospects of our proposed channel, in terms of statistical significance.

Consider the production of heavy RHN, through an off-shell W^\pm . This in a further decay produces relatively clean, same sign di-muon pair $\mu^\pm\mu^\pm$ final states, in association with a boosted W^\pm . Our primary objective is to unmask these W^\pm from other hadronic backgrounds. This is efficiently achieved by utilizing jet substructure to W-tag the fat-jet originating from W^\pm . Of course, one expects from our previous discussions that the fat-jet and jet substructure techniques become significant when W^\pm bosons are generated with sufficient boost. Hence, as mentioned earlier, our primary region of interest is when $M_N \gg M_W$. Notably, these are also the ranges where conventional searches at colliders fail to probe the mixing parameters very effectively. Corresponding to the signal production channel depicted in figure 1, we will consider

$$\begin{aligned} pp &\rightarrow \ell_1^+ N, \quad N \rightarrow \ell_2^+ W^-, \quad W^- \rightarrow J \\ pp &\rightarrow \ell_1^- \bar{N}, \quad \bar{N} \rightarrow \ell_2^- W^+, \quad W^+ \rightarrow J. \end{aligned} \tag{4.1}$$

As mentioned before, for concreteness we assume the light-heavy mixing is non-zero only for the muon flavor in a simplified model. The muons also provide cleaner lepton signals. Hence, all leptons we consider in this study will be muons. It is straightforward to extend the analysis if more lepton flavors are allowed.

Backgrounds for our SSDL+fat-jet channel can originate from electroweak gauge boson decays along with a fat-jet; the latter for instance produced from a W boson decaying to J . Additionally, some of the QCD jets can also mimic J . Hence, one is required to simulate all such processes accompanied by hard jet(s) at the parton level, and then match them with shower jet events.

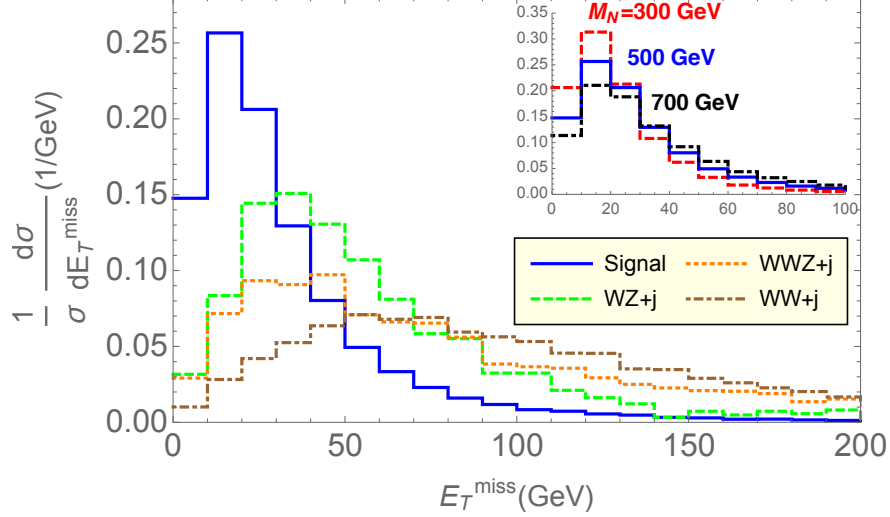


Figure 3. Normalised differential distribution of events as a function of missing transverse momentum, after the application of the basic selection cuts; including $p_T^J > 100$ GeV. The distribution for $M_N = 500$ GeV along with all dominant backgrounds is shown. Inset shows the variations for three benchmark signal points with $M_N = 300, 500$ and 700 GeV.

Dominant contributions come from same-sign W^\pm pair production in association with jets – $W^\pm W^\pm + jets$. Here, W^\pm would decay leptonically. One of these jets has the possibility to resemble a W^\pm -like fat-jet. Another significantly large contribution comes from WZ production, where both vector bosons decay leptonically. Subsequently, one of the charged lepton is missed in the detector, giving an SSDL signature. An additional fat-jet like component can come either from a radiated jet or an associated W^\pm boson decaying hadronically.

We implement the parton level event generation using `MadGraph5-aMC@NLO` [107, 108] and signal model files are generated with `FeynRules` [109, 110]. `CTEQ6L` [111] is adopted for the parton distribution functions (PDF) and the factorization scale μ_F is set to the default MadGraph option. The showering, fragmentation and hadronization of the generated events were performed with `PYTHIA6.4` [112]. The matching is done using the MLM scheme [113]; based on a shower-kT algorithm with pT-ordered showers. For SM backgrounds, the matching scale `Q CUT` is set between 20 and 30 GeV. The showered events are passed through `Delphes 3.3.2` [101] for detector level simulations with the default CMS card. The jets and associated substructure variables are constructed as described in section 3.

To establish specific features and kinematic characteristics related to our RHN signal and backgrounds, we start by focusing on signal identification. Our prototypical signal is Same Flavour (μ^\pm) SSDL, in association with a fat-jet. We adopt the following selection criteria

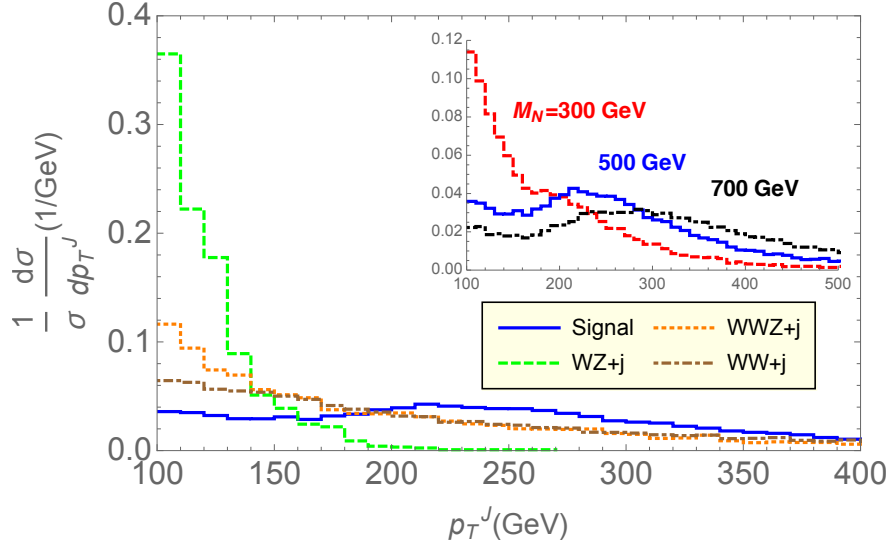


Figure 4. Normalised differential distributions as a function of fat-jet (J) transverse momentum, again after the application of the basic selection cuts. $M_N = 500$ GeV distribution with all dominant backgrounds are shown along with an inset showing the $M_N = 300$, 500 and 700 GeV cases.

- Muons μ^\pm are identified with a minimum transverse momentum $p_T^\mu > 10$ GeV and rapidity range $|\eta^\mu| < 2.4$, with a maximum efficiency of 95%. Efficiency decreases for p_T^μ above 1 TeV.
- Only events with reconstructed di-muons having same sign are selected for further analysis.
- Hard jets having at least $p_T^j > 10$ GeV and $|\eta^j| < 2.4$ are identified.
- Candidate fat-jets are to be identified, following the criteria in section 3 (an $R = 0.8$, CA jet with $|\eta^J| < 2.4$).
- We identify the hardest fat-jet with the W^\pm candidate jet (J), and this is required to have $p_T^J > 100$ GeV.

The above **basic selection criteria** are like primary level cuts required for effective signal identification. The last requirement is to ensure robust fat-jet properties. As argued earlier, features of the boosted fat-jet are rather more prominent for large M_N ; showing up emphatically for 300 GeV and above. In the next section we introduce some additional event criteria and then illustrate various results by considering several signal benchmark points.

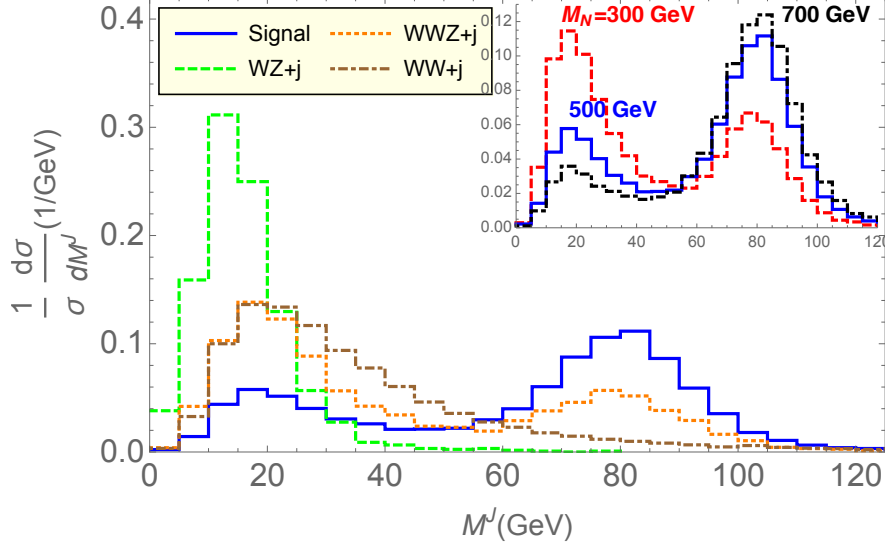


Figure 5. Normalised differential distributions as a function of fat-jet (J) invariant mass in case of same sign di-lepton + fat-jet production channel after the application of the basic selection cuts including $p_T^J > 100$ GeV. Distributions of one signal region with all dominant backgrounds are shown in the plot. Inset shows the variation for three benchmark signal points with $M_N = 300, 500$ and 700 GeV.

5 Results and Discussion

In the previous section, basic selection criteria were set. We are now in a position to identify specific features and kinematic characteristics that can further differentiate RHN events from SM backgrounds. To highlight the differences, we focus on four key characteristic distributions, considering backgrounds along with three signal benchmark points (based on $M_N = 300, 500$ and 700 GeV).

Figure 3 illustrates the normalized differential distribution of events as a function of missing transverse momentum, after the application of the basic selection cuts. Missing transverse momentum (MET) is calculated from the contributions of isolated electrons, muons, photons and jets along with unclustered deposits. Our signal of interest from RHN involves no missing particle at the detector and is thus expected to have low MET. The only MET contributions may be from the mismeasurement of hard jets. On the contrary, in almost all relevant background processes, leptons originate from W^\pm along with a neutrino. The neutrinos are not detected and contribute to a large MET. Distribution of one prototypical signal region with all dominant backgrounds is shown in the plot. It clearly shows the larger MET contribution for the backgrounds. Inset shows the same distribution for three benchmark signal points, $M_N = 300, 500$ and 700 GeV. Distributions are very mildly sensitive to M_N , since heavier masses contribute to harder boosted jets and the jet-energy

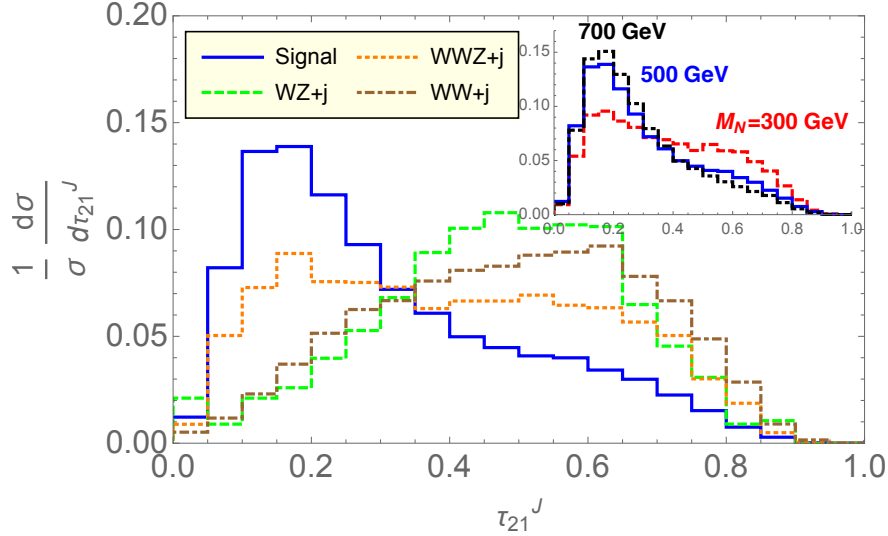


Figure 6. Normalised differential distributions as a function of two to one N-subjet ratio τ_{21}^J for fat-jet (J) in case of same sign di-lepton + fat-jet production channel after the application of the basic selection cuts including $p_T^J > 100$ GeV. Distributions of one signal region with all dominant backgrounds are shown in the plot. Inset shows the variation for three benchmark signal points with $M_N = 300, 500$ and 700 GeV.

mis-measurements have a P_T dependence.

Figure 4 presents the normalized differential distributions for the fat-jet transverse momentum in a similar way. Here, minimum P_T^J of 100 GeV has already been imposed. As we discussed in section 3, P_T^J is the vector sum of all constituent four momenta in J . Signal distribution is noticeably harder compared to background distributions, which fall faster. Comparison of different signal distributions is also quite interesting. As expected, heavier M_N produces harder J candidates.

Imposing a minimum P_T^J selection brings out marked differences in the distribution of M_J and τ_{21}^J , between signal and background events. These jet shape variables can be very powerful in further containing the backgrounds. Two fat-jet invariant mass peaks are evident from the figure 5. Second peak at around 80 GeV reflects the jet mass of W like fat-jet J . This peak is absent for those backgrounds where fat-jet is faked by QCD jets. Only the triple gauge boson background, where fat-jet can originate from hadronic decay of one of the W 's, provide some contamination to signal. The signal plots in the inset are also quite instructive, showing the significant W like fat-jet contributions for higher M_N . The small spurious peak is due to events where some four-momenta from the hadronically decaying boosted- W^\pm is missed in the jet clustering. This spurious peak around 20 GeV may be reduced by imposing a larger P_T^J . This would of course cut down the signal as well, and we find $P_T^J \gtrsim 100$ GeV to provide the most optimal signal significance.

Another excellent discriminant to tag a hadronic two-pronged object is $\tau_{21}^J = \tau_2/\tau_1$, as we discussed in section 3. Corresponding distributions are shown in figure 6. τ_{21}^J for W^\pm -like fat-jets peak around small values and this is clearly visible in figure 6. It becomes more prominent for larger M_N , as the inset figure shows, due to the J being more boosted.

It is important to reemphasize that the choice of a higher, minimum P_T^J effectively selects purer, W^\pm -like fat-jet events, but probably at the cost of some signal. This is essentially reflected in the larger event fractions in the higher (lower) peaks for m^J (τ_{21}^J). This would result in a sharper peak and background reductions. We find $P_T^J > 150$ GeV to be optimal for selecting events, while maintaining good signal significance, as mentioned.

We list below our final event selection criteria motivated by the kinematic distributions.

- Leading muon should have $p_T(\mu_1) > 20$ GeV and the next hardest muon must have $p_T(\mu_2) > 15$ GeV.
- Minimum invariant mass for the same sign muon pair must satisfy $m_{\mu\mu} > 50$ GeV. This is easily satisfied for the signal events, and can control backgrounds with non-prompt muon pairs.
- Lacking any missing particles for our signal, require $E_T^{\text{miss}} < 35$ GeV. This can control background events with large MET contributions.
- The hardest, reconstructed fat-jet must have $p_T^J > 150$ GeV.
- We also demand the invariant mass of the hardest, reconstructed fat-jet to satisfy $M_J > 50$ GeV. In principle one may use a mass window around the W^\pm mass, but we find that a simple lower bound suffices.
- The N-subjettiness ratio corresponding to the reconstructed fat-jet must satisfy $\tau_{21}^J < 0.5$.

With these we are able to achieve very significant background elimination, relative to the signal.

Now we present our results. The effects of the different cuts, as we have motivated, are summarized in Table 1 in the form of a cut-flow. Three reference RHN benchmark points are presented with masses 300 GeV, 500 GeV and 700 GeV. It is quite clear, in reference to the different distributions shown earlier, that the choice of these cuts are extremely efficient in controlling the large SM backgrounds. This enables the RHN signal to be probed to a significant mass range, or alternatively to smaller mixing angles, at the LHC.

Cut	Signal for M_N			Background		
	300 GeV	500 GeV	700 GeV	$WW+j$	$WZ+j$	$WWZ+j$
Pre-selection + $\mu^\pm\mu^\pm + J$	60.0+33.0	26.7+17.4	14.0+9.5	3282.0+3136.5	5474.4+4234.5	126.05+120.2
$p_T^J > 100$ GeV	[100%]	[100%]	[100%]	[100%]	[100%]	[100%]
$p_T(\mu_{1,2}), m_{\mu\mu}$	58.0+ 29.0	24.1+ 14.8	11.4+6.7	2724.30+2575.03	3045.2+2796.2	104.0+96.7
	[94%]	[88%]	[77%]	[83%]	[60%]	[82%]
$E_T^{\text{miss}} < 35$ GeV	48.34+20.0	20.8 +13.2	7.3+5.5	314.94+197.1	105.2+104.2	12.1+ 9.8
	[74%]	[77%]	[55%]	[7.9%]	[2.2%]	[8.9%]
$p_T^J > 150$ GeV	25.6+15.0	15.2+ 10.5	6.0+4.3	184.02+110.4	20.2+ 15.08	7.07+6.2
	[44%]	[58%]	[44%]	[4.5%]	[0.4%]	[5.3%]
$M_J > 50$ GeV	21.4+12.3	11.2+ 7.4	4.8+3.2	41.05+32.08	6.4+4.7	3.3+2.5
	[36%]	[42%]	[34%]	[1.1%]	[0.1%]	[2.3%]
$\tau_{21}^J < 0.5$	19.5+10.0	9.6+5.2	3.9+2.0	21.1+19.3	3.3+2.9	1.5+1.4
	[32%]	[34%]	[25%]	[0.6%]	[0.06%]	[1.2%]

Table 1. The effectiveness of different variables in minimizing backgrounds is illustrated in the form a cut flow. The two numbers correspond to expected events in $\mu^+\mu^+$ and $\mu^-\mu^-$ channels. We adopt a typical mixing angle $|V_{\mu N}| = 0.03$. The numbers are for an integrated luminosity of 3000fb^{-1} , at the 13 TeV LHC.

The statistical significance (\mathcal{S}) of the observed signal events (S) over the total SM background events (B) has been calculated using

$$\mathcal{S} = S/\sqrt{B} \quad \text{for } 5\sigma \text{ significance,} \quad (5.1)$$

$$\mathcal{S} = \sqrt{2 \times \left[(S+B) \ln\left(1 + \frac{S}{B}\right) - S \right]} \quad \text{for } 2\sigma \text{ and } 3\sigma \text{ significance.} \quad (5.2)$$

figure 7 displays the significance contours in the $(M_N, |V_{\mu N}|^2)$ plane. These contours reflect the extensive capability of RHN searches augmented by jet substructure techniques. One obtains interesting limits all the way from $M_N = 300$ GeV with $|V_{\mu N}|^2 = 2.6 \times 10^{-4}$ to $M_N = 800$ GeV with $|V_{\mu N}|^2 = 9.6 \times 10^{-4}$.

It is instructive to compare our projected collider limits with existing LHC limits, as well as indirect EWPD bounds. This is shown in figure 8. There are currently no limits above $M_N = 500$ GeV, from any experiment. From ATLAS searches [17] at $\sqrt{s} = 8$ TeV, the blue solid line shows the limits for the $e^\pm e^\pm jj$ channel and the brown solid line for the $\mu^\pm \mu^\pm jj$ channel. The orange dashed line shows the limits for $e^\pm e^\pm jj$ and the green dot-dashed line shows limits for $\mu^\pm \mu^\pm jj$, both from CMS [18, 19]. The light gray solid line stands for the EWPD limit for μ flavor mixings [20, 23, 81].

Note that our event selection criteria is optimized to the lower side of the heavy neutrino mass and we have applied the same cuts universally for the full signal mass range. Now, we have already observed in the inset plots of Figs. 3-6, that distributions change with M_N . Hence, there is sufficient room left to improve our results for higher M_N , by focused optimizations at each mass point. Instead of fine tuning the analysis, our main aim here was to demonstrate the efficacy and usefulness of jet substructure analysis in the general RHN collider search context [115].

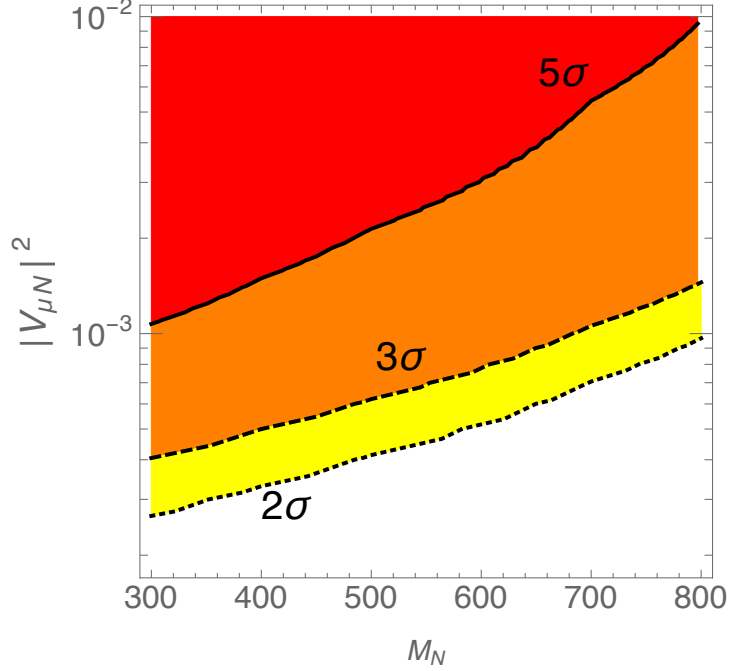


Figure 7. Exclusion limit in terms of heavy neutrino mass M_N and $|V_{\mu N}|^2$ at the 13 TeV LHC.

6 Conclusions

Seesaw models can naturally incorporate the existence of tiny neutrino masses and flavor mixings through simple extensions of the SM, many of which have Majorana RHNs. Such RHNs, if they exist at the TeV scale, can be produced and detected at the LHC. Searches have been performed for these states in the dilepton+dijet channel. Here we propose for the first time a search in the dilepton+fat-jet channel, leveraging jet substructure methods which can very significantly increase the LHC reach for these RHN states. In our case we considered the mass region $M_N \geq 300$ GeV. We used the unique kinematic characteristics of a fat-jet – such as P_T^J , M^J and τ_{21}^J – to W-tag it and it was found that this helps greatly in discriminating the RHN SSDL+fat-jet signal from backgrounds. Exclusion limits are obtained by computing signal significance and the bounds we obtain are many orders of magnitude stronger than current LHC limits.

Acknowledgments

We thank Akanksha Bhardwaj for independent validation of this work and also facilitating JaxoDraw [116, 117] generated diagram.

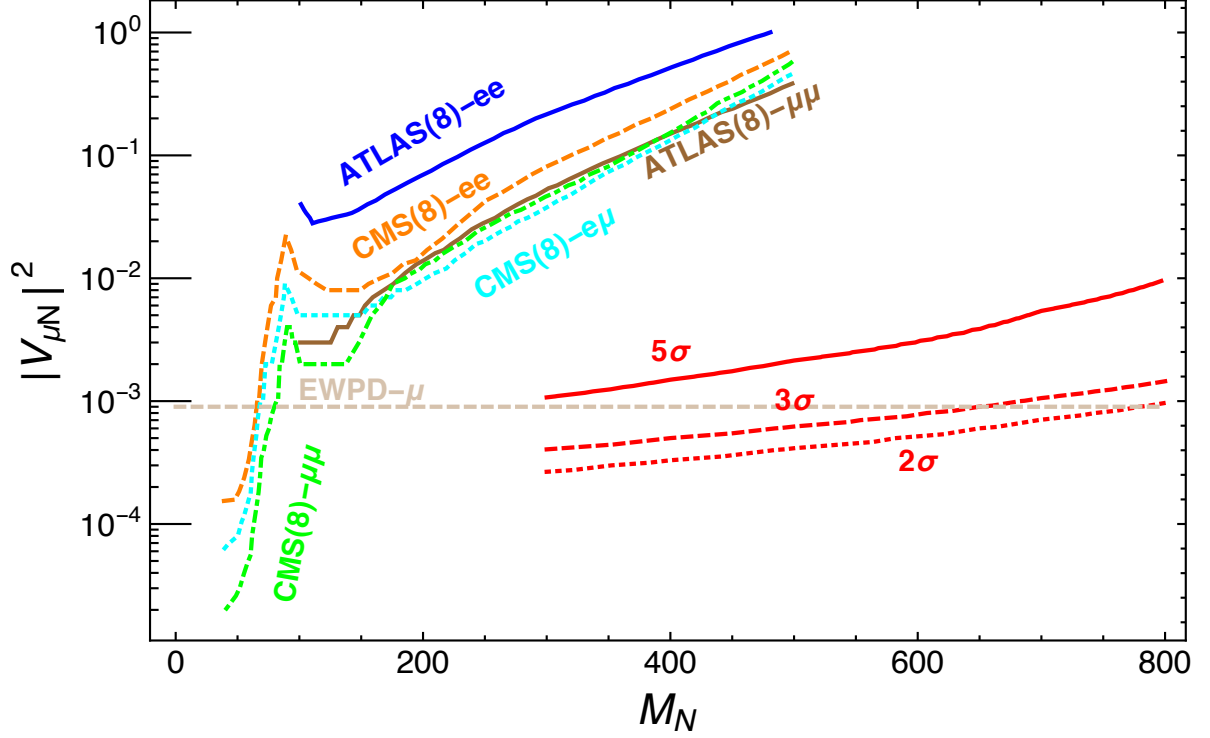


Figure 8. Exclusion limit in terms of heavy neutrino mass M_N and $|V_{\mu N}|^2$ at the 13 TeV LHC with other available limits.

References

- [1] K. Abe et. al. [T2K Collaboration] Phys. Rev. Lett. 107, 041801 (2011).
- [2] P. Adamson et al. [MINOS Collaboration], Phys. Rev. Lett. 107, 181802 (2011).
- [3] Y. Abe et al. [DOUBLE-CHOOZ Collaboration], Phys. Rev. Lett. 108, 131801 (2012).
- [4] F. P. An et al. [DAYA-BAY Collaboration], Phys. Rev. Lett. 108, 171803 (2012).
- [5] J. K. Ahn et al. [RENO Collaboration], Phys. Rev. Lett. 108, 191802 (2012).
- [6] C. Patrignani *et al.* [Particle Data Group], “Review of Particle Physics,” Chin. Phys. C **40**, no. 10, 100001 (2016). doi:10.1088/1674-1137/40/10/100001
- [7] S. Weinberg, “Baryon and Lepton Nonconserving Processes,” Phys. Rev. Lett. **43**, 1566 (1979). doi:10.1103/PhysRevLett.43.1566
- [8] P. Minkowski, “ $\mu \rightarrow e\gamma$ at a Rate of One Out of 10^9 Muon Decays?,” Phys. Lett. **67B**, 421 (1977). doi:10.1016/0370-2693(77)90435-X
- [9] T. Yanagida, “Horizontal Symmetry and Masses of Neutrinos,” Prog. Theor. Phys. **64**, 1103 (1980).

- [10] J. Schechter and J. W. F. Valle, “Neutrino Masses in $SU(2) \otimes U(1)$ Theories,” *Phys. Rev. D* **22**, 2227 (1980).
- [11] T. Yanagida, in Proceedings of the Workshop on the Unified Theory and the Baryon Number in the Universe (O. Sawada and A. Sugamoto, eds.), KEK, Tsukuba, Japan, 1979, p. 95.
- [12] M. Gell-Mann, P. Ramond, and R. Slansky, Supergravity (P. van Nieuwenhuizen et al. eds.), North Holland, Amsterdam, 1979, p. 315.
- [13] S. L. Glashow, The future of elementary particle physics, in Proceedings of the 1979 Cargèse Summer Institute on Quarks and Leptons (M. Levy et al. eds.), Plenum Press, New York, 1980, p. 687.
- [14] R. N. Mohapatra and G. Senjanovic, “Neutrino Mass and Spontaneous Parity Violation,” *Phys. Rev. Lett.* **44**, 912 (1980).
- [15] K. Fujikawa, *Prog. Theor. Phys.* **113** (2005) 1065 doi:10.1143/PTP.113.1065 [hep-ph/0407331].
- [16] A. de Gouvea, *Phys. Rev. D* **72** (2005) 033005 doi:10.1103/PhysRevD.72.033005 [hep-ph/0501039].
- [17] G. Aad *et al.* [ATLAS Collaboration], “Search for heavy Majorana neutrinos with the ATLAS detector in pp collisions at $\sqrt{s} = 8$ TeV,” *JHEP* **1507**, 162 (2015) doi:10.1007/JHEP07(2015)162 [arXiv:1506.06020 [hep-ex]].
- [18] V. Khachatryan *et al.* [CMS Collaboration], “Search for heavy Majorana neutrinos in $e^\pm e^\pm + \text{jets}$ and $e^\pm \mu^\pm + \text{jets}$ events in proton-proton collisions at $\sqrt{s} = 8$ TeV,” *JHEP* **1604**, 169 (2016) doi: 10.1007/JHEP04 (2016)169 [arxiv:1603.02248 [hep-ex]].
- [19] V. Khachatryan *et al.* [CMS Collaboration], “Search for heavy Majorana neutrinos in $\mu^\pm \mu^\pm + \text{jets}$ events in proton-proton collisions at $\sqrt{s} = 8$ TeV,” *Phys. Lett. B* **748**, 144 (2015) doi:10.1016/j.physletb.2015.06.070 [arXiv:1501.05566 [hep-ex]].
- [20] F. del Aguila, J. de Blas and M. Perez-Victoria, “Effects of new leptons in Electroweak Precision Data,” *Phys. Rev. D* **78**, 013010 (2008) doi:10.1103/PhysRevD.78.013010 [arXiv:0803.4008 [hep-ph]].
- [21] J. de Blas, “Electroweak limits on physics beyond the Standard Model,” *EPJ Web Conf.* **60**, 19008 (2013) doi:10.1051/epjconf/20136019008 [arXiv:1307.6173 [hep-ph]].
- [22] A. Gando *et al.* [KamLAND-Zen Collaboration], “Search for Majorana Neutrinos near the Inverted Mass Hierarchy Region with KamLAND-Zen,” *Phys. Rev. Lett.* **117**, no. 8, 082503 (2016) Addendum: [*Phys. Rev. Lett.* **117**, no. 10, 109903 (2016)] doi:10.1103/PhysRevLett.117.109903, 10.1103/PhysRevLett.117.082503 [arXiv:1605.02889 [hep-ex]] .
- [23] E. Akhmedov, A. Kartavtsev, M. Lindner, L. Michaels and J. Smirnov, “Improving

- Electro-Weak Fits with TeV-scale Sterile Neutrinos,” *JHEP* **1305**, 081 (2013) doi:10.1007/JHEP05(2013)081 [arXiv:1302.1872 [hep-ph]].
- [24] P. S. Bhupal Dev, R. Franceschini and R. N. Mohapatra, “Bounds on TeV Seesaw Models from LHC Higgs Data,” *Phys. Rev. D* **86**, 093010 (2012) doi:10.1103/PhysRevD.86.093010 [arXiv:1207.2756 [hep-ph]].
- [25] A. Das, P. S. B. Dev and C. S. Kim, “Constraining Sterile Neutrinos from Precision Higgs Data,” *Phys. Rev. D* **95**, no. 11, 115013 (2017) doi:10.1103/PhysRevD.95.115013 [arXiv:1704.00880 [hep-ph]].
- [26] A. Das, Y. Gao and T. Kamon, “Heavy Neutrino Search via the Higgs boson at the LHC,” arXiv:1704.00881 [hep-ph].
- [27] M. H. Seymour, *Searches for new particles using cone and cluster jet algorithms: A Comparative study*, *Z.Phys.* **C62** (1994) 127–138.
- [28] J. Butterworth, J. R. Ellis, and A. Raklev, *Reconstructing sparticle mass spectra using hadronic decays*, *JHEP* **0705** (2007) 033, [[hep-ph/0702150](#)].
- [29] G. Brooijmans, *High pt hadronic top quark identification*, Tech. Rep. ATL-PHYS-CONF-2008-008. ATL-COM-PHYS-2008-001, CERN, Geneva, Jan, 2008.
- [30] J. M. Butterworth, A. R. Davison, M. Rubin, and G. P. Salam, *Jet substructure as a new Higgs search channel at the LHC*, *Phys.Rev.Lett.* **100** (2008) 242001, [[arXiv:0802.2470](#)].
- [31] D. Adams *et al.*, “Towards an Understanding of the Correlations in Jet Substructure,” *Eur. Phys. J. C* **75** (2015) no.9, 409 doi:10.1140/epjc/s10052-015-3587-2 [arXiv:1504.00679 [hep-ph]].
- [32] E. Izaguirre and B. Shuve, “Multilepton and Lepton Jet Probes of Sub-Weak-Scale Right-Handed Neutrinos,” *Phys. Rev. D* **91** (2015) no.9, 093010 doi:10.1103/PhysRevD.91.093010 [arXiv:1504.02470 [hep-ph]].
- [33] S. Antusch, E. Cazzato and O. Fischer, “Sterile neutrino searches at future e^-e^+ , pp , and e^-p colliders,” arXiv:1612.02728 [hep-ph].
- [34] M. Mitra, R. Ruiz, D. J. Scott and M. Spannowsky, “Neutrino Jets from High-Mass W_R Gauge Bosons in TeV-Scale Left-Right Symmetric Models,” *Phys. Rev. D* **94**, no. 9, 095016 (2016) doi:10.1103/PhysRevD.94.095016 [arXiv:1607.03504 [hep-ph]].
- [35] S. Dube, D. Gadkari and A. M. Thalappilil, “Lepton-Jets and Low-Mass Sterile Neutrinos at Hadron Colliders,” *Phys. Rev. D* **96** (2017) no.5, 055031 doi:10.1103/PhysRevD.96.055031 [arXiv:1707.00008 [hep-ph]].
- [36] P. Cox, C. Han and T. T. Yanagida, “LHC Search for Right-handed Neutrinos in Z' Models,” arXiv:1707.04532 [hep-ph].
- [37] J. A. Casas and A. Ibarra, “Oscillating neutrinos and $\mu\mu\mu \rightarrow e, \gamma$,” *Nucl. Phys. B* **618**, 171 (2001) doi:10.1016/S0550-3213(01)00475-8 [hep-ph/0103065].

- [38] W. Y. Keung and G. Senjanovic, “Majorana Neutrinos and the Production of the Right-handed Charged Gauge Boson,” *Phys. Rev. Lett.* **50**, 1427 (1983).
doi:10.1103/PhysRevLett.50.1427
- [39] A. Datta, M. Guchait and D. P. Roy, “Prospect of heavy right-handed neutrino search at SSC / CERN LHC energies,” *Phys. Rev. D* **47**, 961 (1993)
doi:10.1103/PhysRevD.47.961 [hep-ph/9208228].
- [40] A. Datta, M. Guchait and A. Pilaftsis, “Probing lepton number violation via majorana neutrinos at hadron supercolliders,” *Phys. Rev. D* **50**, 3195 (1994)
doi:10.1103/PhysRevD.50.3195 [hep-ph/9311257].
- [41] J. A. Aguilar-Saavedra, “Heavy lepton pair production at LHC: Model discrimination with multi-lepton signals,” *Nucl. Phys. B* **828**, 289 (2010)
doi:10.1016/j.nuclphysb.2009.11.021 [arXiv:0905.2221 [hep-ph]].
- [42] C. Y. Chen and P. S. B. Dev, “Multi-Lepton Collider Signatures of Heavy Dirac and Majorana Neutrinos,” *Phys. Rev. D* **85**, 093018 (2012)
doi:10.1103/PhysRevD.85.093018 [arXiv:1112.6419 [hep-ph]].
- [43] A. Das and N. Okada, “Inverse seesaw neutrino signatures at the LHC and ILC,” *Phys. Rev. D* **88**, 113001 (2013) doi:10.1103/PhysRevD.88.113001 [arXiv:1207.3734 [hep-ph]].
- [44] A. Das, P. S. Bhupal Dev and N. Okada, “Direct bounds on electroweak scale pseudo-Dirac neutrinos from $\sqrt{s} = 8$ TeV LHC data,” *Phys. Lett. B* **735**, 364 (2014) doi:10.1016/j.physletb.2014.06.058 [arXiv:1405.0177 [hep-ph]].
- [45] A. Das and N. Okada, “Improved bounds on the heavy neutrino productions at the LHC,” *Phys. Rev. D* **93**, no. 3, 033003 (2016) doi:10.1103/PhysRevD.93.033003 [arXiv:1510.04790 [hep-ph]].
- [46] P. S. Bhupal Dev and R. N. Mohapatra, “Unified explanation of the $eejj$, diboson and dijet resonances at the LHC,” *Phys. Rev. Lett.* **115**, no. 18, 181803 (2015)
doi:10.1103/PhysRevLett.115.181803 [arXiv:1508.02277 [hep-ph]].
- [47] A. Das, N. Nagata and N. Okada, “Testing the 2-TeV Resonance with Trileptons,” arXiv:1601.05079 [hep-ph].
- [48] J. Gluza, T. Jelinski and R. Szafron, “Lepton Number Violation and ‘Diracness’ of massive neutrinos composed of Majorana states,” arXiv:1604.01388 [hep-ph].
- [49] F. del Aguila and J. A. Aguilar-Saavedra, “Electroweak scale seesaw and heavy Dirac neutrino signals at LHC,” *Phys. Lett. B* **672**, 158 (2009)
doi:10.1016/j.physletb.2009.01.010 [arXiv:0809.2096 [hep-ph]].
- [50] F. del Aguila, J. A. Aguilar-Saavedra and R. Pittau, “Heavy neutrino signals at large hadron colliders,” *JHEP* **0710**, 047 (2007)
doi:10.1088/1126-6708/2007/10/047 [hep-ph/0703261].
- [51] J. A. Aguilar-Saavedra and F. R. Joaquim, “Measuring heavy neutrino couplings at

- the LHC,” *Phys. Rev. D* **86**, 073005 (2012) doi:10.1103/PhysRevD.86.073005 [arXiv:1207.4193 [hep-ph]].
- [52] B. P. Nayak and M. K. Parida, “Dilepton events with displaced vertices, double beta decay, and resonant leptogenesis with Type-II seesaw dominance, TeV scale Z' and heavy neutrinos,” arXiv:1509.06192 [hep-ph].
 - [53] B. P. Nayak and M. K. Parida, “New mechanism for Type-II seesaw dominance in SO(10) with low-mass Z' , RH neutrinos, and verifiable LFV, LNV and proton decay,” *Eur. Phys. J. C* **75**, 183 (2015) doi:10.1140/epjc/s10052-015-3385-x [arXiv:1312.3185 [hep-ph]].
 - [54] J. A. Aguilar-Saavedra, F. Deppisch, O. Kittel and J. W. F. Valle, “Flavour in heavy neutrino searches at the LHC,” *Phys. Rev. D* **85**, 091301 (2012) doi:10.1103/PhysRevD.85.091301 [arXiv:1203.5998 [hep-ph]].
 - [55] R. Lal Awasthi and M. K. Parida, “Inverse Seesaw Mechanism in Nonsupersymmetric SO(10), Proton Lifetime, Nonunitarity Effects, and a Low-mass Z' Boson,” *Phys. Rev. D* **86**, 093004 (2012) doi:10.1103/PhysRevD.86.093004 [arXiv:1112.1826 [hep-ph]].
 - [56] C. S. Fong, R. N. Mohapatra and I. Sung, “Majorana Neutrinos from Inverse Seesaw in Warped Extra Dimension,” *Phys. Lett. B* **704**, 171 (2011) doi:10.1016/j.physletb.2011.08.069 [arXiv:1107.4086 [hep-ph]].
 - [57] A. G. Dias, C. A. de S. Pires and P. S. R. da Silva, “How the Inverse See-Saw Mechanism Can Reveal Itself Natural, Canonical and Independent of the Right-Handed Neutrino Mass,” *Phys. Rev. D* **84**, 053011 (2011) doi:10.1103/PhysRevD.84.053011 [arXiv:1107.0739 [hep-ph]].
 - [58] A. Ibarra, E. Molinaro and S. T. Petcov, “Low Energy Signatures of the TeV Scale See-Saw Mechanism,” *Phys. Rev. D* **84**, 013005 (2011) doi:10.1103/PhysRevD.84.013005 [arXiv:1103.6217 [hep-ph]].
 - [59] T. Saito *et al.*, “Extra dimensions and Seesaw Neutrinos at the International Linear Collider,” *Phys. Rev. D* **82**, 093004 (2010) [arXiv:1008.2257 [hep-ph]].
 - [60] S. Banerjee, P. S. B. Dev, A. Ibarra, T. Mandal and M. Mitra, “Prospects of Heavy Neutrino Searches at Future Lepton Colliders,” arXiv:1503.05491 [hep-ph].
 - [61] F. del Aguila, J. A. Aguilar-Saavedra and R. Pittau, “Heavy neutrino signals at large hadron colliders,” *JHEP* **0710**, 047 (2007) [hep-ph/0703261].
 - [62] F. del Aguila and J. A. Aguilar-Saavedra, “Distinguishing seesaw models at LHC with multi-lepton signals,” *Nucl. Phys. B* **813**, 22 (2009) [arXiv:0808.2468 [hep-ph]].
 - [63] B. Batell and M. McCullough, “Neutrino Masses from Neutral Top Partners,” *Phys. Rev. D* **92**, no. 7, 073018 (2015) doi:10.1103/PhysRevD.92.073018 [arXiv:1504.04016 [hep-ph]].
 - [64] R. Leonardi, L. Alunni, F. Romeo, L. Fano and O. Panella, “Hunting for heavy composite Majorana neutrinos at the LHC,” arXiv:1510.07988 [hep-ph].

- [65] P. S. B. Dev, A. Pilaftsis, U. K. Yang, Phys. Rev. Lett. 112 (2014) 081801, arXiv:1308.2209 [hep-ph].
- [66] G. Bambhaniya, S. Khan, P. Konar and T. Mondal, “Constraints on a seesaw model leading to quasidegenerate neutrinos and signatures at the LHC,” Phys. Rev. D **91**, no. 9, 095007 (2015) [arXiv:1411.6866 [hep-ph]].
- [67] G. Bambhaniya, S. Goswami, S. Khan, P. Konar and T. Mondal, “Looking for hints of a reconstructible seesaw model at the Large Hadron Collider,” Phys. Rev. D **91**, 075007 (2015) [arXiv:1410.5687 [hep-ph]].
- [68] G. Dutta and A. S. Joshipura, “PseudoDirac neutrinos in seesaw model,” Phys. Rev. D **51**, 3838 (1995) doi:10.1103/PhysRevD.51.3838 [hep-ph/9405291].
- [69] N. Haba, S. Matsumoto and K. Yoshioka, “Observable Seesaw and its Collider Signatures,” Phys. Lett. B **677**, 291 (2009) doi:10.1016/j.physletb.2009.05.042 [arXiv:0901.4596 [hep-ph]].
- [70] S. Matsumoto, T. Nabeshima and K. Yoshioka, “Seesaw Neutrino Signals at the Large Hadron Collider,” JHEP **1006**, 058 (2010) doi:10.1007/JHEP06(2010)058 [arXiv:1004.3852 [hep-ph]].
- [71] S. Mondal, S. Biswas, P. Ghosh and S. Roy, “Exploring novel correlations in trilepton channels at the LHC for the minimal supersymmetric inverse seesaw model,” JHEP **1205**, 134 (2012) doi:10.1007/JHEP05(2012)134 [arXiv:1201.1556 [hep-ph]].
- [72] J. C. Helo, M. Hirsch and S. Kovalenko, “Heavy neutrino searches at the LHC with displaced vertices,” Phys. Rev. D **89**, 073005 (2014) doi:10.1103/PhysRevD.89.073005 [arXiv:1312.2900 [hep-ph]].
- [73] A. G. Hessler, A. Ibarra, E. Molinaro and S. Vogl, “Impact of the Higgs boson on the production of exotic particles at the LHC,” Phys. Rev. D **91**, no. 11, 115004 (2015) doi:10.1103/PhysRevD.91.115004 [arXiv:1408.0983 [hep-ph]].
- [74] F. F. Deppisch, P. S. Bhupal Dev and A. Pilaftsis, “Neutrinos and Collider Physics,” New J. Phys. **17**, no. 7, 075019 (2015) doi:10.1088/1367-2630/17/7/075019 [arXiv:1502.06541 [hep-ph]].
- [75] E. Arganda, M. J. Herrero, X. Marcano and C. Weiland, “Exotic $\mu\tau jj$ events from heavy ISS neutrinos at the LHC,” Phys. Lett. B **752**, 46 (2016) doi:10.1016/j.physletb.2015.11.013 [arXiv:1508.05074 [hep-ph]].
- [76] C. O. Dib and C. S. Kim, “Discovering sterile Neutrinos lighter than M_W at the LHC,” Phys. Rev. D **92**, no. 9, 093009 (2015) doi:10.1103/PhysRevD.92.093009 [arXiv:1509.05981 [hep-ph]].
- [77] A. Das and N. Okada, “Bounds on heavy Majorana neutrinos in type-I seesaw and implications for collider searches,” arXiv:1702.04668 [hep-ph].
- [78] J. Adam *et al.* [MEG Collaboration], “New limit on the lepton-flavour violating

- decay $\mu^+ \rightarrow e^+ \gamma$,” Phys. Rev. Lett. **107**, 171801 (2011)
doi:10.1103/PhysRevLett.107.171801 [arXiv:1107.5547 [hep-ex]].
- [79] B. Aubert *et al.* [BaBar Collaboration], “Searches for Lepton Flavor Violation in the Decays $\tau^+ \rightarrow e^+ \gamma$ and $\tau^+ \rightarrow \mu^+ \gamma$,” Phys. Rev. Lett. **104**, 021802 (2010) doi:10.1103/PhysRevLett.104.021802 [arXiv:0908.2381 [hep-ex]].
- [80] B. O’Leary *et al.* [SuperB Collaboration], “SuperB Progress Reports – Physics,” arXiv:1008.1541 [hep-ex].
- [81] P. Achard *et al.* [L3 Collaboration], “Search for heavy isosinglet neutrino in e^+e^- annihilation at LEP,” Phys. Lett. B **517**, 67 (2001)
doi:10.1016/S0370-2693(01)00993-5 [hep-ex/0107014].
- [82] S. Antusch, C. Biggio, E. Fernandez-Martinez, M. B. Gavela and J. Lopez-Pavon, “Unitarity of the Leptonic Mixing Matrix,” JHEP **0610**, 084 (2006)
doi:10.1088/1126-6708/2006/10/084 [hep-ph/0607020].
- [83] A. Abada, C. Biggio, F. Bonnet, M. B. Gavela and T. Hambye, “Low energy effects of neutrino masses,” JHEP **0712**, 061 (2007) doi:10.1088/1126-6708/2007/12/061 [arXiv:0707.4058 [hep-ph]].
- [84] N. Okada, Y. Orikasa and T. Yamada, “Minimal Flavor Violation in the Minimal $U(1)_{B-L}$ Model and Resonant Leptogenesis,” Phys. Rev. D **86**, 076003 (2012)
doi:10.1103/PhysRevD.86.076003 [arXiv:1207.1510 [hep-ph]].
- [85] A. Ibarra, E. Molinaro and S. T. Petcov, “TeV Scale See-Saw Mechanisms of Neutrino Mass Generation, the Majorana Nature of the Heavy Singlet Neutrinos and $(\beta\beta)_{0\nu}$ -Decay,” JHEP **1009**, 108 (2010) doi:10.1007/JHEP09(2010)108 [arXiv:1007.2378 [hep-ph]].
- [86] D. N. Dinh, A. Ibarra, E. Molinaro and S. T. Petcov, “The $\mu - e$ Conversion in Nuclei, $\mu \rightarrow e \gamma$, $\mu \rightarrow 3e$ Decays and TeV Scale See-Saw Scenarios of Neutrino Mass Generation,” JHEP **1208**, 125 (2012) Erratum: [JHEP **1309**, 023 (2013)]
doi:10.1007/JHEP09(2013)023, 10.1007/JHEP08(2012)125 [arXiv:1205.4671 [hep-ph]].
- [87] R. W. Rasmussen and W. Winter, “Perspectives for tests of neutrino mass generation at the GeV scale: Experimental reach versus theoretical predictions,” Phys. Rev. D **94**, no. 7, 073004 (2016) doi:10.1103/PhysRevD.94.073004 [arXiv:1607.07880 [hep-ph]].
- [88] B. Pontecorvo, “Inverse beta processes and nonconservation of lepton charge,” Sov. Phys. JETP **7**, 172 (1958) [Zh. Eksp. Teor. Fiz. **34**, 247 (1957)].
- [89] Z. Maki, M. Nakagawa and S. Sakata, “Remarks on the unified model of elementary particles,” Prog. Theor. Phys. **28**, 870 (1962). doi:10.1143/PTP.28.870
- [90] A. Pilaftsis and T. E. J. Underwood, “Resonant leptogenesis,” Nucl. Phys. B **692**, 303 (2004) doi:10.1016/j.nuclphysb.2004.05.029 [hep-ph/0309342].

- [91] J. Kersten and A. Y. Smirnov, “Right-Handed Neutrinos at CERN LHC and the Mechanism of Neutrino Mass Generation,” *Phys. Rev. D* **76**, 073005 (2007) doi:10.1103/PhysRevD.76.073005 [arXiv:0705.3221 [hep-ph]].
- [92] Z. z. Xing, “Naturalness and Testability of TeV Seesaw Mechanisms,” *Prog. Theor. Phys. Suppl.* **180**, 112 (2009) doi:10.1143/PTPS.180.112 [arXiv:0905.3903 [hep-ph]].
- [93] X. G. He, S. Oh, J. Tandean and C. C. Wen, “Large Mixing of Light and Heavy Neutrinos in Seesaw Models and the LHC,” *Phys. Rev. D* **80**, 073012 (2009) doi:10.1103/PhysRevD.80.073012 [arXiv:0907.1607 [hep-ph]].
- [94] F. F. Deppisch and A. Pilaftsis, “Lepton Flavour Violation and $\theta(13)$ in Minimal Resonant Leptogenesis,” *Phys. Rev. D* **83**, 076007 (2011) doi:10.1103/PhysRevD.83.076007 [arXiv:1012.1834 [hep-ph]].
- [95] C. H. Lee, P. S. Bhupal Dev and R. N. Mohapatra, “Natural TeV-scale left-right seesaw mechanism for neutrinos and experimental tests,” *Phys. Rev. D* **88**, no. 9, 093010 (2013) doi:10.1103/PhysRevD.88.093010 [arXiv:1309.0774 [hep-ph]].
- [96] J. Pumplin, D. R. Stump, J. Huston, H. L. Lai, P. M. Nadolsky and W. K. Tung, “New generation of parton distributions with uncertainties from global QCD analysis,” *JHEP* **0207**, 012 (2002) doi:10.1088/1126-6708/2002/07/012 [hep-ph/0201195].
- [97] A. Das, P. Konar and S. Majhi, “Production of Heavy neutrino in next-to-leading order QCD at the LHC and beyond,” *JHEP* **1606**, 019 (2016) doi:10.1007/JHEP06(2016)019 [arXiv:1604.00608 [hep-ph]].
- [98] A. Das, “Pair production of heavy neutrinos in next-to-leading order QCD at the hadron colliders in the inverse seesaw framework,” arXiv:1701.04946 [hep-ph].
- [99] J. Thaler and K. Van Tilburg, “Identifying Boosted Objects with N-subjettiness,” *JHEP* **1103**, 015 (2011) doi:10.1007/JHEP03(2011)015 [arXiv:1011.2268 [hep-ph]].
- [100] J. Thaler and K. Van Tilburg, “Maximizing Boosted Top Identification by Minimizing N-subjettiness,” *JHEP* **1202**, 093 (2012) doi:10.1007/JHEP02(2012)093 [arXiv:1108.2701 [hep-ph]].
- [101] J. de Favereau *et al.* [DELPHES 3 Collaboration], “DELPHES 3, A modular framework for fast simulation of a generic collider experiment,” *JHEP* **1402** (2014) 057 doi:10.1007/JHEP02(2014)057 [arXiv:1307.6346 [hep-ex]].
- [102] M. Cacciari, G. P. Salam and G. Soyez, “FastJet user manual,” *Eur. Phys. J. C* **72** (2012) 1896 [arXiv:1111.6097 [hep-ph]].
- [103] M. Cacciari and G. P. Salam, “Dispelling the N^3 myth for the k_t jet-finder,” *Phys. Lett. B* **641** (2006) 57 [hep-ph/0512210].
- [104] V. Khachatryan *et al.* [CMS Collaboration], “Identification techniques for highly boosted W bosons that decay into hadrons,” *JHEP* **1412**, 017 (2014) doi:10.1007/JHEP12(2014)017 [arXiv:1410.4227 [hep-ex]].

- [105] Y. L. Dokshitzer, G. D. Leder, S. Moretti, and B. R. Webber, *Better Jet Clustering Algorithms*, *JHEP* **08** (1997) 001, [[hep-ph/9707323](#)].
- [106] M. Wobisch and T. Wengler, *Hadronization corrections to jet cross sections in deep- inelastic scattering*, [hep-ph/9907280](#).
- [107] J. Alwall, M. Herquet, F. Maltoni, O. Mattelaer and T. Stelzer, “MadGraph 5 : Going Beyond,” *JHEP* **1106**, 128 (2011)[[arXiv:1106.0522 \[hep-ph\]](#)].
- [108] J. Alwall, M. Herquet, F. Maltoni, O. Mattelaer, T. Stelzer, *J. High Energy Phys.* **1106** (2011) 128, [arXiv: 1106.0522 \[hep-ph\]](#)
- [109] N. D. Christensen and C. Duhr, “FeynRules - Feynman rules made easy,” *Comput. Phys. Commun.* **180**, 1614 (2009) doi:10.1016/j.cpc.2009.02.018 [[arXiv:0806.4194 \[hep-ph\]](#)].
- [110] A. Alloul, N. D. Christensen, C. Degrande, C. Duhr and B. Fuks, “FeynRules 2.0 - A complete toolbox for tree-level phenomenology,” *Comput. Phys. Commun.* **185**, 2250 (2014) doi:10.1016/j.cpc.2014.04.012 [[arXiv:1310.1921 \[hep-ph\]](#)].
- [111] J. Pumplin, D. R. Stump, J. Huston, H. L. Lai, P. M. Nadolsky and W. K. Tung, “New generation of parton distributions with uncertainties from global QCD analysis,” *JHEP* **0207**, 012 (2002) doi:10.1088/1126-6708/2002/07/012 [[hep-ph/0201195](#)].
- [112] T. Sjostrand, S. Mrenna and P. Z. Skands, “PYTHIA 6.4 Physics and Manual,” *JHEP* **0605**, 026 (2006) doi:10.1088/1126-6708/2006/05/026 [[hep-ph/0603175](#)].
- [113] S. Hoeche, F. Krauss, N. Lavesson, L. Lonnblad, M. Mangano, A. Schalicke and S. Schumann, “Matching parton showers and matrix elements,” doi:10.5170/CERN-2005-014.288 [hep-ph/0602031](#).
- [114] M. Cacciari, G. P. Salam and G. Soyez, “The Anti-k(t) jet clustering algorithm,” *JHEP* **0804**, 063 (2008) doi:10.1088/1126-6708/2008/04/063 [[arXiv:0802.1189 \[hep-ph\]](#)].
- [115] Akanksha Bhardwaj, Arindam Das, Partha Konar, Arun Thalappillil, in preparation.
- [116] D. Binosi and L. Theussl, “JaxoDraw: A Graphical user interface for drawing Feynman diagrams,” *Comput. Phys. Commun.* **161**, 76 (2004) doi:10.1016/j.cpc.2004.05.001 [[hep-ph/0309015](#)].
- [117] D. Binosi, J. Collins, C. Kaufhold and L. Theussl, “JaxoDraw: A Graphical user interface for drawing Feynman diagrams. Version 2.0 release notes,” *Comput. Phys. Commun.* **180**, 1709 (2009) doi:10.1016/j.cpc.2009.02.020 [[arXiv:0811.4113 \[hep-ph\]](#)].